ORIGINAL ARTICLE

WILEY | Cell Proliferation

Transient receptor potential melastatin 4 channel is required for rat dental pulp stem cell proliferation and survival

T.D. Ngoc Tran[1]* | K.E. Stovall[1]* | T. Suantawee[2] | Y. Hu[1] | S. Yao[1] (iD) | L.-J. Yang[3] |
S. Adisakwattana[4] | H. Cheng[1] (iD)

[1]Department of Comparative Biomedical Sciences, School of Veterinary Medicine, Louisiana State University, Baton Rouge, LA, USA

[2]Program in Biomedical Sciences, Graduate School, Chulalongkorn University, Bangkok, Thailand

[3]Department of Pathology, Immunology and Laboratory Medicine, University of Florida College of Medicine, Gainesville, FL, USA

[4]Department of Nutrition and Dietetics, Faculty of Allied Health Sciences, Chulalongkorn University, Bangkok, Thailand

Correspondence
Henrique Cheng, Department of Comparative Biomedical Sciences, School of Veterinary Medicine, Louisiana State University, Baton Rouge, LA, USA.
Email: hcheng@lsu.edu

Abstract

Objectives: Investigate the role of the transient receptor potential melastatin 4 (TRPM4) channel in rat dental pulp stem cell (DPSC) proliferation and survival.

Materials and methods: Immunofluorescence and FACS analysis were used to detect the stem cell marker CD90. Alizarin Red S and Oil Red O staining were used to identify osteoblast and adipocyte differentiation, respectively. To characterize TRPM4, patch-clamp recordings were obtained from single cells in the whole-cell configuration mode. The significance of TRPM4 for proliferation and survival was examined with 9-phenanthrol, a TRPM4 inhibitor during a 96-hour period of culture. Real-time Ca^{2+} imaging analysis with Fura-2AM was used to investigate the impact of TRPM4 on intracellular Ca^{2+} signals.

Results: DPSCs were CD90-positive and differentiated into osteoblasts. Patch-clamp recordings revealed currents typical of TRPM4 that were Ca^{2+}-activated, voltage-dependent and Na^+-conducting. Inhibition of TRPM4 resulted in a significant reduction in the cell population after a 96-hr period of culture and transformed the biphasic pattern of intracellular Ca^{2+} signalling into sustained oscillations.

Conclusions: Rat DPSCs have stem cell characteristics and functional TRPM4 channels that are required for proliferation and survival. These data suggest that the shape and frequency of intracellular Ca^{2+} signals may mediate stem cell proliferation and survival.

1 | INTRODUCTION

Dental pulp stem cells (DPSCs) of mesenchymal origin are a potential source of stem cells capable of differentiating into specialized tissues.[1,2] They can differentiate into osteoblasts to promote the repair and regeneration of alveolar bone defects[3] and grow into dental pulp-like tissue in a matrix of dentin.[4] When cultured on a perforated collagen scaffold, DPSCs differentiate into odontoblast-like cells in the presence of Dentin Matrix Acidic Phosphoprotein-1.[5] Nam et al. reported odontoblastic differentiation and dentin deposition when DPSCs were grown on porous granules of Ca^{2+} phosphate, even in the absence of induction.[6] In vivo experiments have shown that in combination with a collagen scaffold and DMP-1, these cells can regenerate dentin in perforated molars.[7] Other studies have revealed that DPSCs can be used in the repair or treatment of non-dental tissues because they develop into new bone when injected into defective regions of the mandible.[8] DPSC co-culture with mesencephalic neurons reduces neuronal destruction from MPP+ and rotenone in a model for Parkinson's disease.[9] In addition, DPSCs can enhance wound healing[10] and differentiate into neural progenitor cells,[11] odontoblasts and endothelial cells.[12] The process of stem cell proliferation and differentiation is controlled by a network of intracellular signalling pathways triggered by hormones, ion channels, cytokines, and/or growth factors. Despite reports on the use of DPSCs for tissue regeneration, the mechanisms controlling cell proliferation and survival are not fully understood.

*Equal contributors.

Transient receptor potential (TRP) proteins are a family of ion channels that control intracellular Ca^{2+} signals by conducting Ca^{2+} directly into cells or by controlling the activity of other Ca^{2+} channels such as voltage-dependent calcium channels (VDCCs) or store-operated channels (SOCs).[13] TRPM4, a member of the melastatin family, inhibits osteogenesis but is required for the adipogenesis of dental follicle stem cells (DFSCs).[14] These effects are linked to changes in intracellular Ca^{2+} signals during the differentiation process. Undifferentiated stem cells are considered non-excitable in nature and rely on SOCs for Ca^{2+} influx. In these cells, TRPM4 depolarization due to Na^+ conductivity inhibits Ca^{2+} influx through SOCs. Therefore, TRPM4 suppression increases Ca^{2+} entry, which is observed in DFSCs, immune and neuronal cells.[15–17] The opposite effect is seen in excitable cells (e.g., pancreatic α- and β-cells) where TRPM4-mediated depolarization activates VDCCs.[18,19] In this case, inhibition of TRPM4 decreases Ca^{2+} entry because depolarization is required for the opening of VDCCs. The presence of VDCCs in rat DPSCs was reported by Ju et al. and is necessary for neuron and osteoblast differentiation.[20] Another family member, TRPM7, is a Ca^{2+}- and Mg^{2+}-permeable channel that is essential for cell proliferation and survival.[21] Inhibition of TRPM7 in bone marrow stem cells results in cell death.[22] Deletion of the TRPM7 gene in zebrafish before and during organogenesis results in severe developmental abnormalities,[23] and channel mutation leads to abnormal skeletogenesis, kidney stone formation, albinism and embryonic lethality.[24] In the current study, we characterized, for the first time, the TRPM4 channel in DPSCs and determined its impact on cell proliferation and survival.

2 | MATERIALS AND METHODS

2.1 | Reagents

All reagents were purchased from Sigma Chemical Co. (St. Louis, MO, USA) and ThermoFisher Scientific (Waltham, MA, USA), except FBS (Atlanta Biologicals, Flowery Branch, GA, USA).

2.2 | Dental pulp stem cell isolation and culture

Rat dental pulp was harvested from mandibular molars of 5-7-day post-natal Sprague-Dawley rats and trypsinized to obtain a cell suspension. Cells were grown in α-MEM with 20% FBS and incubated at 37°C and 5% CO_2. At 90% confluence, cells were harvested using Trypsin-EDTA and passaged into a T-75 flask with an initial density of 2×10^5 cells. Primary cultures were tested for their multipotent capability in osteogenic and adipogenic medium prior to experimentation. Cells between passages 2-6 were used.

2.3 | Immunofluorescence and FACS analysis of CD90

For live-cell staining, cells were seeded in a 24-well plate, and the CD90-APC antibody was added to each well at a concentration of 0.6 μg/mL and incubated at 37°C for 30 minutes. Next, the medium with the antibody was aspirated, and the wells were washed twice to remove any unbound antibody. Finally, 0.5 mL of medium was added to each well, and cells were examined using a Zoe Fluorescence Cell Imager (Bio-Rad, Hercules, CA, USA).

For cell sorting, cells were cultured in a T-75 flask to approximately 90% confluency and trypsinized for detachment. Cells were then centrifuged at 704 × g for 5 minutes. The pellet was re-suspended in 5 mL of PBS, passed through a 70 μm filter and centrifuged. After the pellet was washed with PBS, it was suspended in 200 μL PBS, and the CD90-APC antibody was added at a concentration of 0.6 μg/mL. After 30 minutes, cells were centrifuged and washed with PBS to remove any unbound antibody. The cells were re-suspended in PBS to a density of 1×10^6 cells per 100 μL for FACS using an Aria dual laser flow cytometer (BD Biosciences, San Jose, CA, USA). Cells not incubated with the CD90 antibody were used as the negative control.

2.4 | Osteoblast and adipocyte differentiation

The osteogenic medium was formulated with DMEM-LG supplemented with 10% FBS, 10 nmol/L dexamethasone, 0.1 mmol/L ascorbic-acid-2-phosphate and 10 mmol/L β-glycerophosphate. The medium was changed every 4 days during osteogenesis. After 14 days, the medium was aspirated, and the cultures were washed twice with PBS, fixed with 10% formaldehyde, washed again with distilled water and incubated with 1% Alizarin Red S (ARS) in dH_2O. After incubation, the staining solution was removed, and the cultures were washed with distilled water to remove excess dye. Stained monolayers were visualized by phase-contrast microscopy with an inverted microscope (Zeiss, Thornwood, NY, USA).

The adipogenic medium was formulated with DMEM-LG supplemented with 10% FBS, 50 μg/mL ascorbic acid, 0.1 μmol/L dexamethazone and 50 μg/mL indomethacin. After 21 days, lipid droplet accumulation was detected by Oil Red O (ORO) staining. Cells were washed with PBS, fixed with 10% formalin for 10 minutes, washed twice with dH_2O and incubated with 60% isopropanol for 5 minutes. Cells were stained with ORO solution for 5 minutes and washed to remove excess dye. The presence of lipid droplets was visualized by phase-contrast microscopy with an inverted microscope (Zeiss).

2.5 | Electrophysiology

Patch-clamp experiments were performed with external solutions containing (in mmol/L) 140 NaCl, 2.8 KCl, 1 $CaCl_2$, 2 $MgCl_2$, 4 glucose, and 10 HEPES-NaOH, pH 7.2 adjusted with NaOH. The internal solution contained (in mmol/L) 120 Cs-glutamate, 8 NaCl, 1 $MgCl_2$, 10 Cs-BAPTA, 10 HEPES-CsOH, pH 7.2 adjusted with CsOH. Different intracellular buffered Ca^{2+} concentrations were obtained by adjusting the $CaCl_2$ in the internal solution (calculated with WebMaxC http://www.stanford.edu/~cpatton/webmaxcS.htm). The Na^+-free modified Ringer's solution contained (in mmol/L) 140 N-methyl-D-glucamine (NMDG), 2.8 KCl, 1 $CaCl_2$, 2 $MgCl_2$, 4 glucose, 10 HEPES-CsOH, pH 7.2 adjusted with CsOH. For TRPM7 recording, $MgCl_2$ was absent from the internal solution and was prepared according to previous method.[22] All solutions had an osmolarity of ~300 mOsm/L. TRPM4 currents were recorded in the tight-seal whole-cell configuration mode at room temperature. High-resolution

current recordings were acquired using a computer-based patch-clamp amplifier system (EPC-10; HEKA, Lambrecht, Germany). Patch pipettes had resistances of 3-5 MΩ and were coated in Sigmacote® silicon solution (Sigma-Aldrich). Following the establishment of the whole-cell configuration, 50-ms voltage ramps spanning the voltage range of −100 to +100 mV at a rate of 0.5 Hz over a period of 400-600 s were applied. All voltages were corrected for a liquid junction potential of 10 mV between the external and internal solutions, calculated with Igor PPT Liquid Junction Potential software (Wavemetrics, Portland, OR, USA).

2.6 | Determination of cell proliferation and survival

The Alamar Blue assay was utilized as a non-toxic method to continuously monitor cell growth. Cells were seeded into six-well plates, and experiments were performed at 0, 24, 48, 72 and 96 hour of culture in the presence or absence of the channel inhibitor. At the respective time, the culture medium was removed from each well, and assay medium containing 10% Alamar Blue was added. After 2 hour of incubation, 100 μL assay medium was pipetted into a well of a 96-well plate in triplicate for each sample. Fresh culture and assay medium were used as controls. The plate was placed in a microplate reader model

550 (Bio-Rad), and OD values were obtained. The Alamar Blue reduction was calculated according to the manufacturer's formula.

## 2.7 | Real-time calcium imaging analysis

Cells were loaded with 2 μmol/L Fura-2AM for 30 minutes at 37°C. The imaging buffer containing (in mmol/L) 136 NaCl, 4.8 KCl, 1.2 $CaCl_2$, 1.2 $MgSO_4$, 10 HEPES, 4 glucose and 0.1% BSA, pH 7.3, was used for Fura-2AM loading and perfusion throughout the experiments. Calcium measurements were obtained using a dual excitation fluorometric imaging system (TILL-Photonics, Gräfefingen, Germany) controlled by TILLvisION software. Fura-2AM-loaded cells in the perfusion chamber were excited by 340 and 380 nm wavelengths. Fluorescence emissions were sampled at a frequency of 1 Hz and computed into relative ratio units of the fluorescence intensity of the difference of wavelengths (F340/F380).

2.8 | Data analysis

Cell proliferation was analysed using ANOVA and SAS® software (SAS Institute Inc., Cary, NC, USA) to determine the effects of treatment
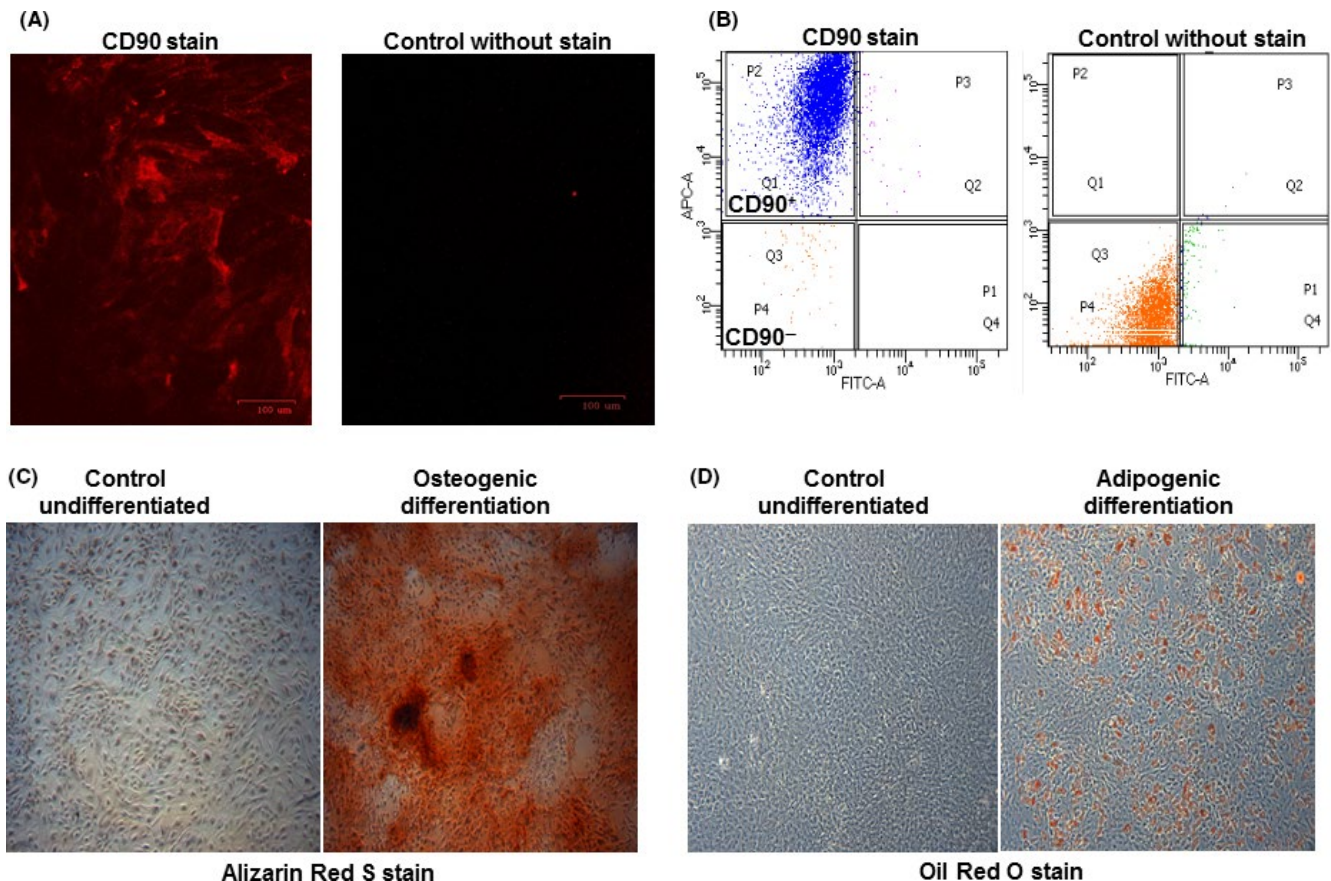

FIGURE 1 DPSCs express the stem cell marker CD90 and differentiate into osteoblasts and adipocytes. A, Cells stained with the CD90-APC antibody were shown to be CD90^{+} compared to control unstained cells. B, FACS analysis revealed that the majority of DPSCs (98% of the population) were CD90^{+}. C, Alizarin Red S staining from cells cultured in control growth or osteogenic medium confirmed the Ca^{2+} deposition in the extracellular matrix and mineralization. D, Oil Red O staining from cells cultured in control growth or adipogenic medium show the lipid droplet accumulation in the intracellular space. Images taken at 50X magnification
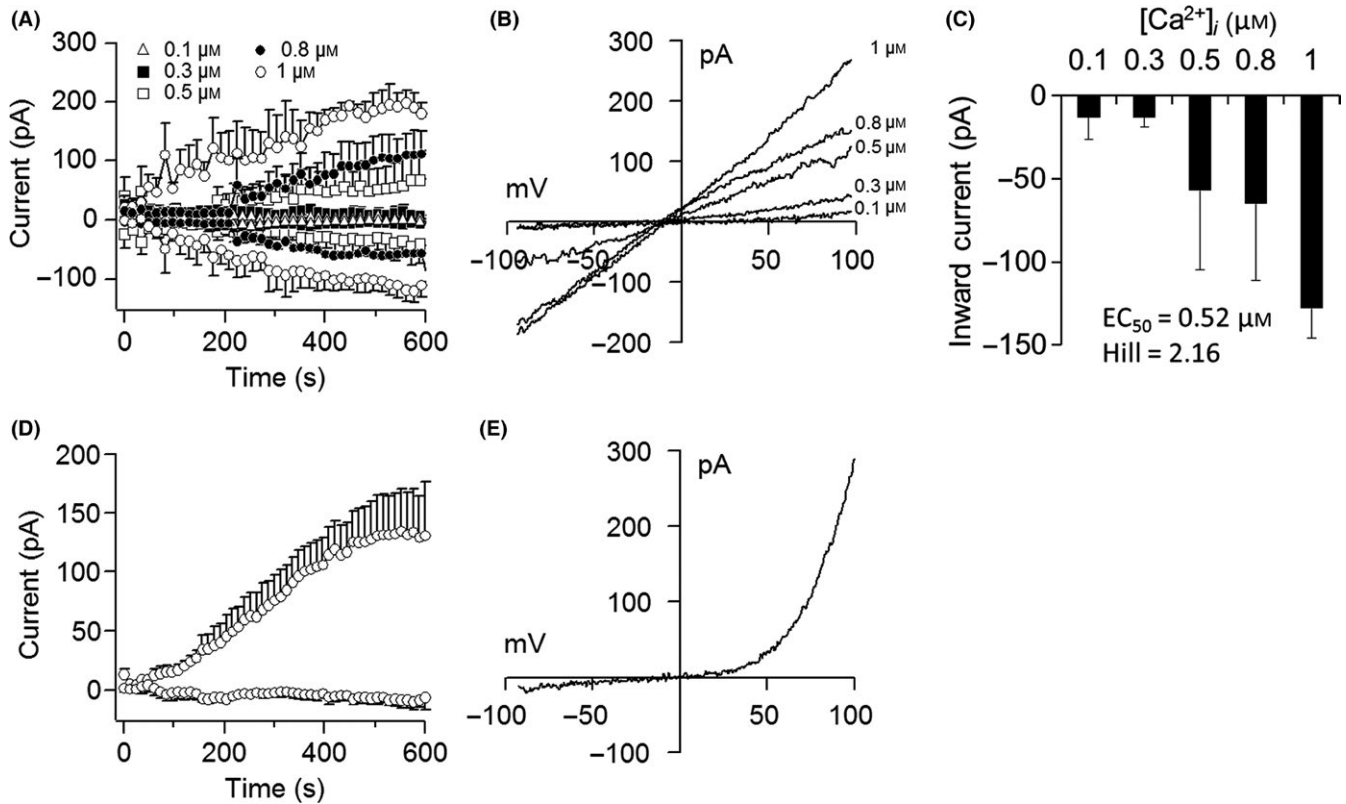
FIGURE 2 TRPM4 channel currents in DPSCs. (A) Patch-clamp recordings from single cells showing the average inward and outward currents during intracellular perfusion with increasing concentrations of buffered Ca^{2+}. Traces represent the mean±SEM (n=3-8 cells/concentration) recorded at a 0-mV holding potential. (B) Current-voltage relationship (I/V) under the experimental conditions described in (A) taken from representative cells at 600 s. (C) Average peak inward currents reflecting Na^+ influx from cells described in (A). (D) Average TRPM7 currents in the absence of $MgCl_2$ in the internal solution. Traces represent the mean±SEM (n=6 cells/concentration). (E) Current-voltage relationship (I/V) under experimental conditions described in (D) taken from representative cells at 600 s
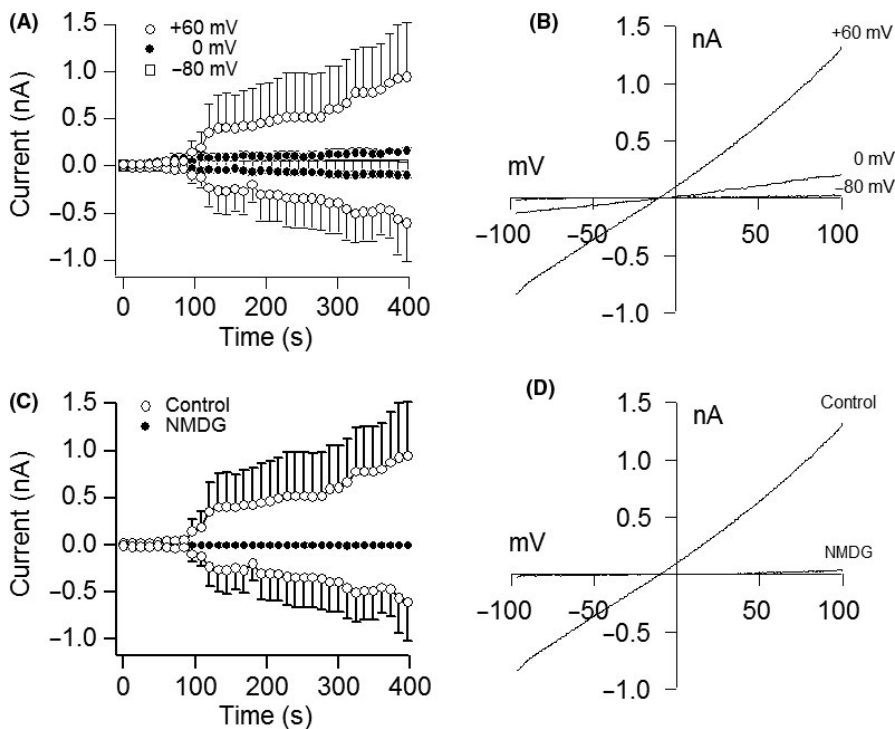
FIGURE 3 Voltage dependency and Na^+ conductivity of TRPM4. A, Average inward and outward currents in response to 1 μmol/L buffered Ca^{2+} at holding potentials of −80, 0 and +60 mV. Traces are mean±SEM (n=3-5 cells/group). B, Current-voltage relationship (I/V) under experimental conditions described above and obtained at 400 s from representative cells at their peak current amplitude. C, Average inward and outward currents in control buffer containing NaCl compared to those in cells maintained in buffer with NMDG replacing NaCl. Experiment was performed with 1 μmol/L buffered Ca^{2+} at a +60-mV holding potential. Traces are mean±SEM (n=4-5 cells/group). D, Current-voltage relationship (I/V) taken at 400 s from representative cells
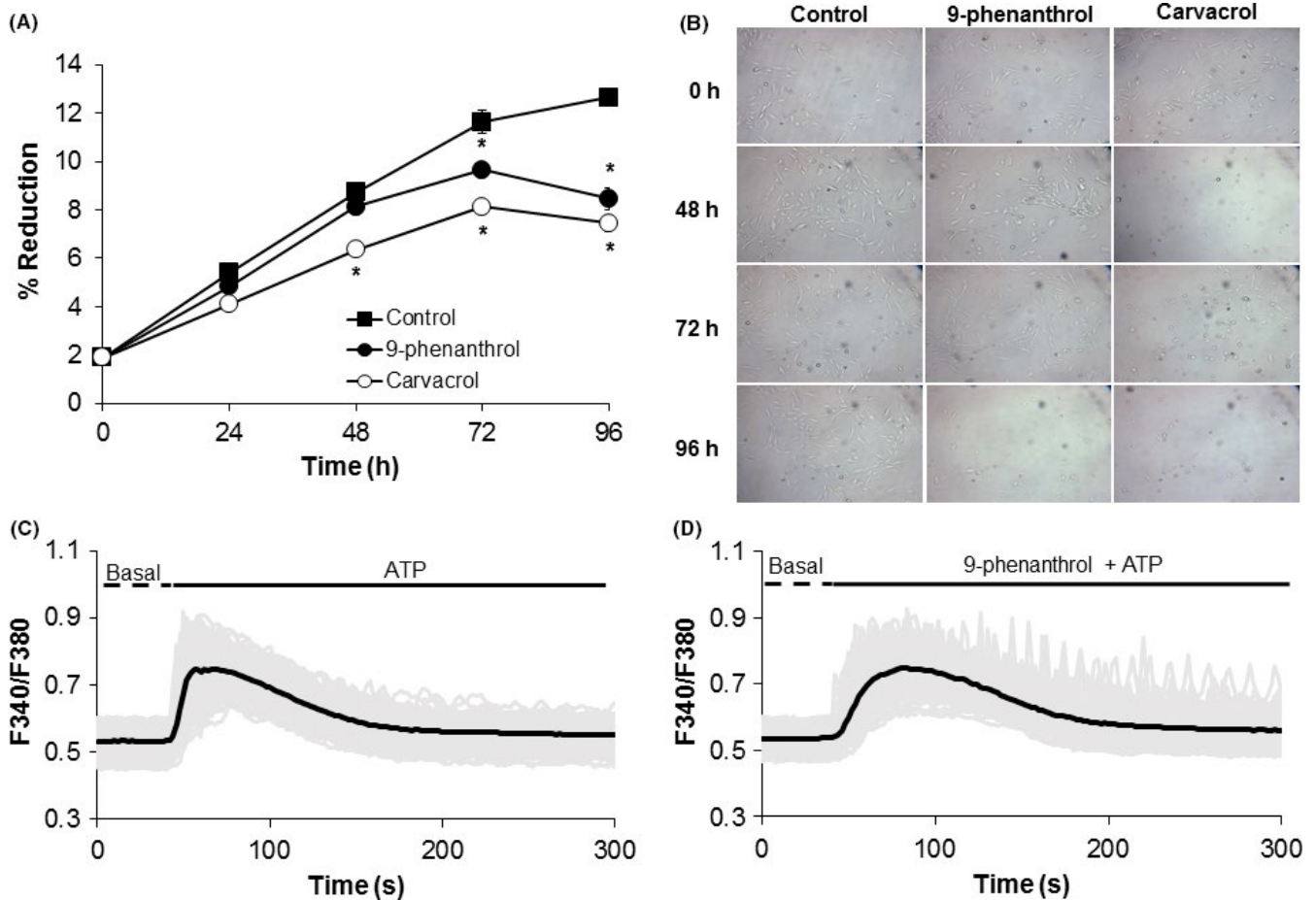
FIGURE 4 Inhibition of TRPM4 decreases DPSC proliferation and survival. A, Average percent reduction in Alamar Blue after 0, 24, 48, 72, and 96 h of culturing cells in growth medium in the absence or presence of the TRPM4 inhibitor 9-phenanthrol (10 µmol/L) or TRPM7 inhibitor carvacrol (300 µmol/L). Experiments were performed in triplicate (3 wells/group). *$P<.05$ compared to control cells in the absence of the inhibitor at the same time point. B, Representative bright-field images during a 96-h period from three independent experiments at 10X magnification. C, Stimulation with 300 µmol/L ATP increased intracellular Ca^{2+} characterized by a first phase due to ER release followed by a secondary phase due to influx. D, Pretreatment of cells with 10 µmol/L 9-phenanthrol prior to ATP stimulation transformed the secondary phase into oscillations. Black line=average from all cells; Gray line=single cell trace. Data represent the average from 125-196 cells/group from three independent experiments

and time. Statistical significance was established at $P<.05$. Calcium imaging data are shown as averages from several cells or representative traces from single cells from three independent experiments.

3 | RESULTS

3.1 | DPSCs are CD90+ and can differentiate into osteoblasts and adipocytes

Immunofluorescence with the CD90-APC stem cell antibody revealed CD90+ cells compared to that observed in control cells in the absence of the antibody (Figure 1A). To quantify the percentage of cells that were CD90+, FACS was used. The results indicated that approximately 98% were CD90+ (Figure 1B). Next, we tested their multipotency with osteogenic and adipogenic medium. Alizarin Red S staining on day 14 detected the presence of calcium deposition in the extracellular matrix (Figure 1C), and Oil Red O staining on day 21 detected the presence

of lipid droplet accumulation (Figure 1D) compared to those in control cells maintained in growth medium.

3.2 | TRPM4 channels are present in DPSCs

Patch-clamp recording in single cells was performed to determine if currents characteristic of TRPM4 currents could be detected.[14,25] Intracellular perfusion with increasing buffered Ca^{2+} concentrations (0.1-1 µmol/L) resulted in a concentration-dependent activation of TRPM4 currents with its signature current-voltage relationship (I/V) (Figure 2A,B). The peak inward currents that depolarized cells with Na^+ influx were obtained with a Ca^{2+} concentration of 1 µmol/L, EC_{50} of 0.52 µmol/L, and Hill coefficient of 2.16 (Figure 2C). We also detected the presence of TRPM7 currents in the absence of $MgCl_2$ in the internal solution (Figure 2D,E). The additional biophysical properties of TRPM4 in DPSCs observed included its voltage dependency and ionic conductivity (Figure 3).
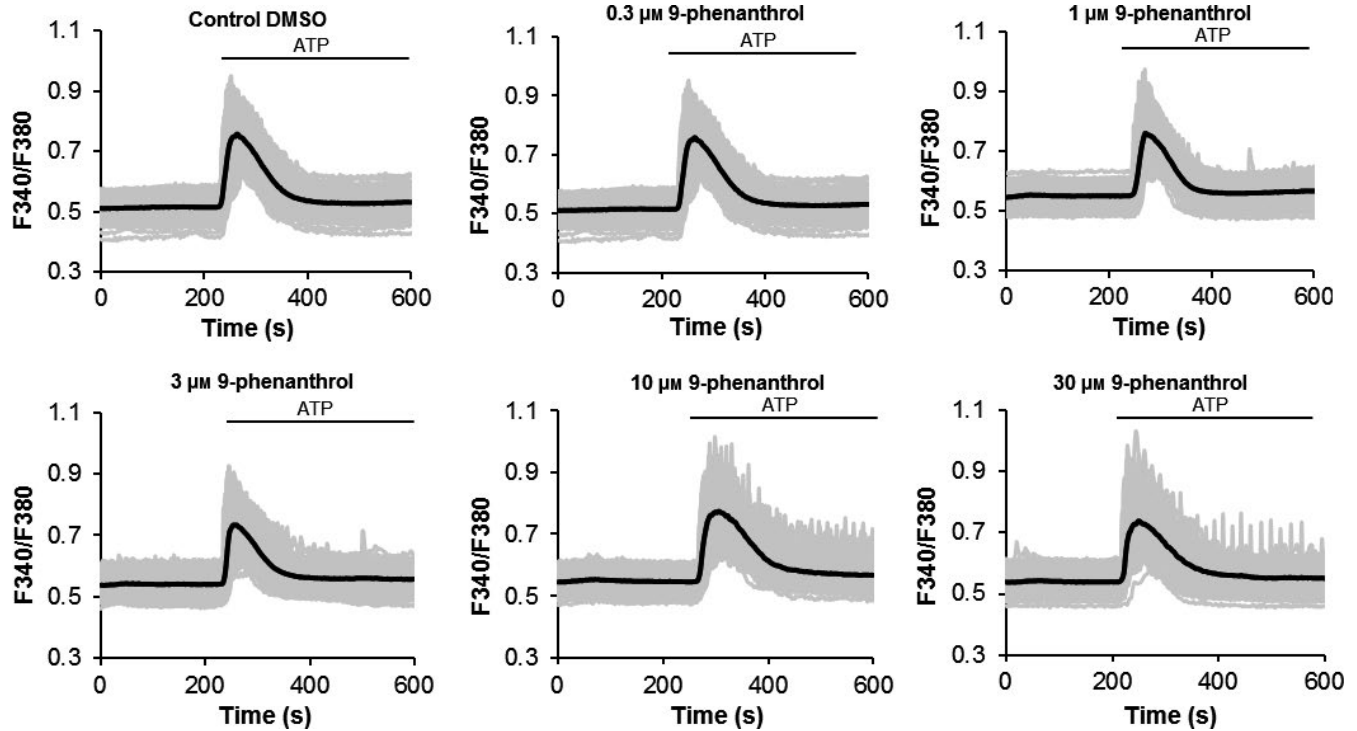
FIGURE 5 Dose–response for 9-phenanthrol during Ca^{2+} imaging analysis. Pretreatment of cells with the TRPM4 blocker 9-phenanthrol (0.3-30 μmol/L) induced intracellular Ca^{2+} oscillations in a concentration-dependent manner during 300 μmol/L ATP stimulation. Black line=average from all cells; Grey line=single cell trace. Data represent the average from 115-168 cells/group from three independent experiments
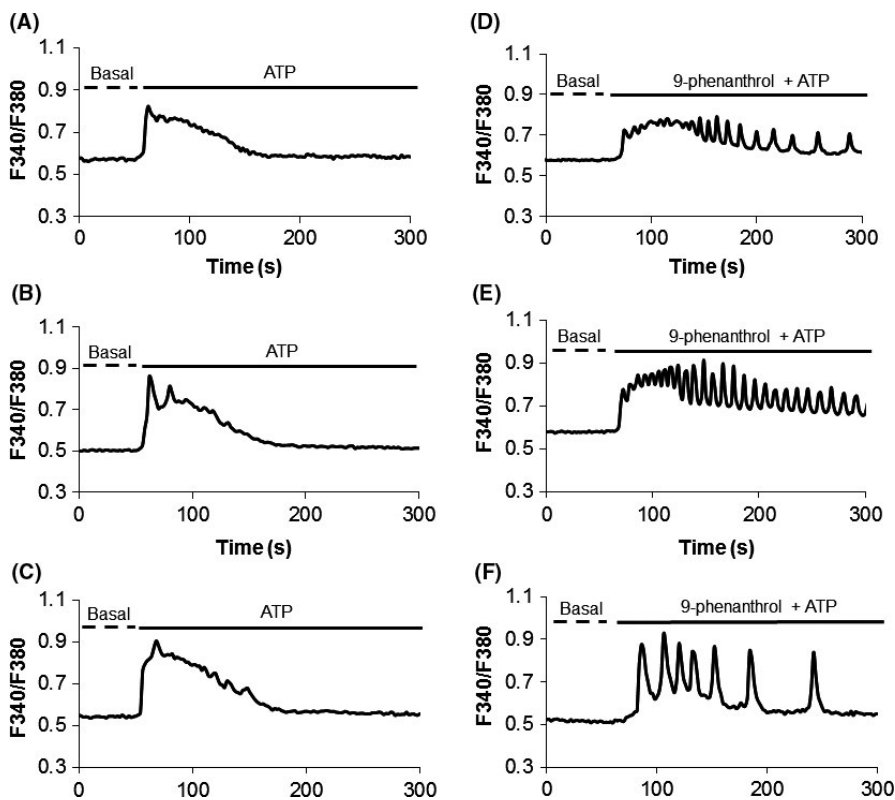
FIGURE 6 Inhibition of TRPM4 induces Ca^{2+} oscillations in DPSCs. (A-C) Representative intracellular Ca^{2+} traces from single cells in response to 300 μmol/L ATP simulation alone. Note the biphasic pattern due to ER release followed by influx from the extracellular space. (D-F) Cells pretreated with 9-phenanthrol (10 μmol/L) followed by 300 μmol/L ATP stimulation reveal the change in the Ca^{2+} signalling pattern

Intracellular perfusion with buffered Ca^{2+} at a 1 μmol/L concentration and holding potential of −80 mV inhibited channel activation, whereas a holding potential of +60 mV facilitated it (Figure 3A,B).

To confirm that the TRPM4 currents were due to Na^+ influx, we substituted NaCl in the extracellular buffer solution for an equimolar concentration of NMDG, which abolished the channel currents

even under 1 μmol/L buffered Ca^{2+} and a +60-mV holding potential (Figure 3C,D).

3.3 | TRPM4 is required for DPSC proliferation and survival

To investigate the impact of TRPM4 on cell proliferation and survival, we utilized the TRPM4 inhibitor 9-phenanthrol.[26] We also examined the effect of TRPM7 suppression using the channel inhibitor carvacrol[27] to confirm its requirement for cell proliferation and survival.[21,28] Inhibition of TRPM4 with 10 μmol/L 9-phenanthrol added to the culture medium reduced cell proliferation and survival at 72 hour of culture but as early as 48 hour with TRPM7 suppression by 300 μmol/L carvacrol compared to that in control cells in the absence of the inhibitor (Figure 4A,B).

3.4 | TRPM4 suppression induces Ca^{2+} oscillations

To determine the impact of TRPM4 on Ca^{2+} signals, cells were pretreated with 9-phenanthrol (10 μmol/L) for 20 minutes followed by ATP (300 μmol/L) stimulation. Inhibition of TRPM4 transformed the Ca^{2+} signalling pattern from biphasic in control cells without 9-phenanthrol (Figure 4C) to sustained oscillations in the presence of the inhibitor (Figure 4D). The presence of these oscillatory signals was observed with an increase in the 9-phenanthrol concentrations from 0.3 to 30 μmol/L (Figure 5). The change in the Ca^{2+} signalling pattern was seen in representative traces from control single cells without the TRPM4 blocker (Figure 6A-C) compared to that seen in cells pretreated with 10 μmol/L 9-phenanthrol (Figure 6C,D).

4 | DISCUSSION

We investigated, for the first time, TRPM4 in DPSCs, which are a potential source of stem cells for tissue regeneration. We detected the stem marker CD90 and could differentiate these cells into osteoblasts and adipocytes. Based on the biophysical properties of the TRPM4 current, it was evident that the current was Ca^{2+}-activated, voltage-dependent, Na^+-conducting and exhibited an I/V typical for the channel.[25] Consistent with most reports, TRPM4 activation was obtained with Ca^{2+} concentrations ranging from 100 nmol/L to 1 μmol/L, thus the calculated EC_{50} and Hill coefficient suggested a greater sensitivity to intracellular Ca^{2+} changes than in other cell types. The effect of voltage on the TRPM4 current was evidenced by the change dependent on the holding potential, where −80 mV inhibited and +60 mV facilitated channel activation. When examining its ionic conductivity, replacement of NaCl in the extracellular buffer for NMDG abolished TRPM4 currents, indicating that Na^+ is necessary for channel function.

The requirement of TRPM4 for DPSC proliferation and survival is in agreement with reports in HeLa cells, a cervical cancer-derived cell line.[29] This mechanism involves the GSK-3β-dependent degradation of β-catenin and reduced β-catenin/Tcf/Lef-dependent transcription. The fact that TRPM4 was needed for DPSC proliferation and survival along with the observation in DFSCs that proliferation is also reduced during osteogenesis and adipogenesis[14] suggests a requirement for TRPM4 during growth and the transition into the differentiation stage. Other studies have revealed that the channel controls the migration of prostate cancer and dendritic cells.[17,30] In prostate cancer, inhibition of TRPM4 reduces migration but not proliferation of DU145 and PC3 cell lines, which may be due to their tumour characteristics.[30] As expected, inhibition of TRPM7 in DPSCs resulted in a significant decrease in cell proliferation and survival as reported in other cell types.

To determine whether intracellular Ca^{2+} signals could be involved in the effect of TRPM4 on DPSC proliferation and survival, we utilized the purinergic receptor agonist ATP that binds to P2Y receptors and activates the PLC-IP_3 pathway to promote Ca^{2+} release from the ER and Ca^{2+} influx. Interestingly, when TRPM4 was inhibited by 9-phenanthrol, the secondary phase of the Ca^{2+} signals due to Ca^{2+} influx was transformed into oscillations. This was unexpected since, in non-excitable cells (e.g., immune and DFSCs), there is generally a gradual and sustained increase.[14,15,31] Although the net Ca^{2+} influx is also increased with oscillations, whether 9-phenanthrol affects the activity of downstream components such as SOCs remains to be determined. TRPM4 mediated-cell depolarization inhibits Ca^{2+} influx via SOCs[31]; therefore, the oscillatory signals most likely reflect changes in the activity of one or both channels. Regarding the electrical nature of DPSCs, undifferentiated stem cells are thought to be non-excitable. However, DPSCs have VDCCs of the $Ca_{v1.2}$ type, which is the main pathway for Ca^{2+} influx in excitable cells.[20] This is in line with our findings in undifferentiated human adipose-derived stem cells that express the $Ca_{v1.2}$.[32] The excitable or non-excitable nature of DPSCs remains to be determined.

In conclusion, these results demonstrate that rat DPSCs have the stem cell marker CD90 and can differentiate into osteoblast and adipocytes. They also have channel currents with characteristics of those for TRPM4. Furthermore, TRPM4 suppression decreased cell proliferation and survival. This regulatory role could be mediated by intracellular Ca^{2+} signalling.

CONFLICT OF INTEREST

The authors do not have any conflicts of interest to declare.

REFERENCES

1. Gronthos S, Brahim J, Li W, et al. Stem cell properties of human dental pulp stem cells. *J Dent Res*. 2002;81:531-535.
2. Zhang W, Walboomers XF, Van Kuppevelt TH, et al. In vivo evaluation of human dental pulp stem cells differentiated towards multiple lineages. *J Tissue Eng Regen Med*. 2008;2:117-125.

3. Jahanbin A, Rashed R, Alamdari DH, et al. Success of maxillary alveolar defect repair in rats using osteoblast-differentiated human deciduous dental pulp stem cells. *J Oral Maxillofac Surg*. 2016;74:829.

4. Gronthos S, Mankani M, Brahim J, Robey PG, Shi S. Postnatal human dental pulp stem cells (DPSCs) in vitro and in vivo. *Proc Natl Acad Sci USA*. 2000;97:13625-13630.

5. Alsanea R, Ravindran S, Fayad MI, et al. Biomimetic approach to perforation repair using dental pulp stem cells and dentin matrix protein 1. *J Endod*. 2011;37:1092-1097.

6. Nam S, Won JE, Kim CH, Kim HW. Odontogenic differentiation of human dental pulp stem cells stimulated by the calcium phosphate porous granules. *J Tissue Eng*. 2011;2011:812547.

7. Prescott RS, Alsanea R, Fayad MI, et al. In vivo generation of dental pulp-like tissue by using dental pulp stem cells, a collagen scaffold, and dentin matrix protein 1 after subcutaneous transplantation in mice. *J Endod*. 2008;34:421-426.

8. Yamada Y, Ito K, Nakamura S, Ueda M, Nagasaka T. Promising cell-based therapy for bone regeneration using stem cells from deciduous teeth, dental pulp, and bone marrow. *Cell Transplant*. 2011;20:1003-1013.

9. Nesti C, Pardini C, Barachini S, et al. Human dental pulp stem cells protect mouse dopaminergic neurons against MPP+ or rotenone. *Brain Res*. 2011;1367:94-102.

10. Nishino Y, Yamada Y, Ebisawa K, et al. Stem cells from human exfoliated deciduous teeth (SHED) enhance wound healing and the possibility of novel cell therapy. *Cytotherapy*. 2011;13:598-605.

11. Nourbakhsh N, Soleimani M, Taghipour Z, et al. Induced in vitro differentiation of neural-like cells from human exfoliated deciduous teeth-derived stem cells. *Int J Dev Biol*. 2011;55:189-195.

12. Sakai VT, Zhang Z, Dong Z, et al. SHED differentiate into functional odontoblasts and endothelium. *J Dent Res*. 2010;89:791-796.

13. Nelson PL, Beck A, Cheng H. Transient receptor proteins illuminated: current views on TRPs and disease. *Vet J*. 2011;187:153-164.

14. Nelson P, Ngoc Tran TD, Zhang H, et al. Transient receptor potential melastatin 4 channel controls calcium signals and dental follicle stem cell differentiation. *Stem Cells*. 2013;31:167-177.

15. Weber KS, Hildner K, Murphy KM, Allen PM. Trpm4 differentially regulates Th1 and Th2 function by altering calcium signaling and NFAT localization. *J Immunol*. 2010;185:2836-2846.

16. Serafini N, Dahdah A, Barbet G, et al. The TRPM4 channel controls monocyte and macrophage, but not neutrophil, function for survival in sepsis. *J Immunol*. 2012;189:3689-3699.

17. Barbet G, Demion M, Moura IC, et al. The calcium-activated nonselective cation channel TRPM4 is essential for the migration but not the maturation of dendritic cells. *Nat Immunol*. 2008;9:1148-1156.

18. Marigo V, Courville K, Hsu WH, Feng JM, Cheng H. TRPM4 impacts on Ca2+ signals during agonist-induced insulin secretion in pancreatic beta-cells. *Mol Cell Endocrinol*. 2009;299:194-203.

19. Nelson PL, Zolochevska O, Figueiredo ML, et al. Regulation of Ca(2+)-entry in pancreatic alpha-cell line by transient receptor potential melastatin 4 plays a vital role in glucagon release. *Mol Cell Endocrinol*. 2011;335:126-134.

20. Ju Y, Ge J, Ren X, et al. Cav1.2 of L-type calcium channel is a key factor for the differentiation of dental pulp stem cells. *J Endod*. 2015;41:1048-1055.

21. Schmitz C, Perraud AL, Johnson CO, et al. Regulation of vertebrate cellular Mg2+ homeostasis by TRPM7. *Cell*. 2003;114:191-200.

22. Cheng H, Feng JM, Figueiredo ML, et al. Transient receptor potential melastatin type 7 channel is critical for the survival of bone marrow derived mesenchymal stem cells. *Stem Cells Dev*. 2010;19:1393-1403.

23. Jin J, Wu LJ, Jun J, et al. The channel kinase, TRPM7, is required for early embryonic development. *Proc Natl Acad Sci USA*. 2012;109:E225-E233.

24. Elizondo MR, Arduini BL, Paulsen J, et al. Defective skeletogenesis with kidney stone formation in dwarf zebrafish mutant for trpm7. *Curr Biol*. 2005;15:667-671.

25. Launay P, Fleig A, Perraud AL, Scharenberg AM, Penner R, Kinet JP. TRPM4 is a Ca2+-activated nonselective cation channel mediating cell membrane depolarization. *Cell*. 2002;109:397-407.

26. Guinamard R, Hof T, Del Negro CA. The TRPM4 channel inhibitor 9-phenanthrol. *Br J Pharmacol*. 2014;171:1600-1613.

27. Parnas M, Peters M, Dadon D, et al. Carvacrol is a novel inhibitor of Drosophila TRPL and mammalian TRPM7 channels. *Cell Calcium*. 2009;45:300-309.

28. Nadler MJ, Hermosura MC, Inabe K, et al. LTRPC7 is a Mg.ATP-regulated divalent cation channel required for cell viability. *Nature*. 2001;411:590-595.

29. Armisen R, Marcelain K, Simon F, et al. TRPM4 enhances cell proliferation through up-regulation of the beta-catenin signaling pathway. *J Cell Physiol*. 2011;226:103-109.

30. Holzmann C, Kappel S, Kilch T, et al. Transient receptor potential melastatin 4 channel contributes to migration of androgen-insensitive prostate cancer cells. *Oncotarget*. 2015;6:41783-41793.

31. Launay P, Cheng H, Srivatsan S, Penner R, Fleig A, Kinet JP. TRPM4 regulates calcium oscillations after T cell activation. *Science*. 2004;306:1374-1377.

32. Tran TD, Zolochevska O, Figueiredo ML, et al. Histamine-induced Ca(2)(+) signalling is mediated by TRPM4 channels in human adipose-derived stem cells. *Biochem J*. 2014;463:123-134.